NITRIC OXIDE SYNTHASE AND NAD(P)H OXIDASE MODULATE CORONARY ENDOTHELIAL CELL GROWTH

Ulvi Bayraktutan DVM, PhD

Department of Medicine, Institute of Clinical Science, Queen's University Belfast, Belfast, United Kingdom

Short title: Free radicals regulate endothelial cell growth

Address for correspondence

Dr Ulvi BAYRAKTUTAN

Department of Medicine,

Institute of Clinical Science Block B,

Queen's University Belfast,

Grosvenor Road,

Belfast BT12 6BJ

United Kingdom

Tel: 00 44 2890 632742

Fax: 00 44 2890 329899

E-mail: u.bayraktutan@qub.ac.uk

Abstract

Reactive oxygen species (ROS) including nitric oxide (NO) and superoxide anion (O_2^-) are associated with cell migration, proliferation and many growth-related diseases. The objective of this study was to determine whether there was a reciprocal relationship between rat coronary microvascular endothelial cell (CMEC) growth and activity/expressions (mRNA and protein) of endothelial NO synthase (eNOS) and NAD(P)H oxidase enzymes. Proliferating namely, 50% confluent CMEC possessed approximately three-fold increased activity and expression of both enzymes compared to 100% confluent cells. Treatment of CMEC with an inhibitor of eNOS (L-NAME, 100 μM) increased cell proliferation as assessed via three independent methods i.e. cell counting, determination of total cellular protein levels and [^{3}H]thymidine incorporation. Similarly, treatment of CMEC with pyrogallol (0.3-3 mM), a superoxide anion (O_2^-)-generator, also increased CMEC growth while spermine NONOate (SpNO), a NO donor, significantly reduced cell growth. Co-incubation of CMEC with a cell permeable superoxide dismutase mimetic (Mn-III-tetrakis-4-benzoic acid-porphyrin; MnTBAP) plus either pyrogallol or NO did not alter cell number and DNA synthesis thereby dismissing the involvement of peroxynitrite ($OONO^-$) in CMEC proliferation. Specific inhibitors of NAD(P)H oxidase but not other ROS-generating enzymes including cyclooxygenase and xanthine oxidase, attenuated cell growth. Transfection of CMEC with antisense p22-phox cDNA, a membrane-bound component of NAD(P)H oxidase, resulted in substantial reduction in [^{3}H]thymidine incorporation, total cellular protein levels and expression of p22-phox protein. These data demonstrate a cross-talk between CMEC growth and eNOS and NAD(P)H oxidase enzyme activity and expression, thus suggesting that the regulation of these enzymes may be critical in preventing the initiation and/or progression of coronary atherosclerosis.

1. Introduction

The vascular endothelium, a multifunctional organ that covers the entire inner surface of all the blood vessels, generates a wide array of vasoactive substances including nitric oxide (NO) in response to several chemical, physical or hormonal stimuli [1]. The integrity of the endothelial layer is preserved by controlled proliferation and migration of endothelial cells in a number of physiological processes such as angiogenesis and during wound healing after an injury to the vascular wall [2,3]. However, in several pathological conditions e.g. tumor metastasis and atherosclerosis endothelial cells proliferate and migrate at greater levels and in an uncontrolled manner [4,5].

NO is generated from amino acid L-arginine within the normal endothelium by endothelial type of NO synthase (eNOS). Although eNOS is constitutively expressed, its expression and activity are mediated by many physio-pathological processes e.g. while shear stress increases its expression in cultured endothelial cells, hypoxia elicits a decrease in eNOS expression/activity [6,7]. NO plays significant roles in the regulation of vascular tone, in the modulation of endothelial cell permeability and in the inhibition of vascular smooth muscle cell (VSMC) proliferation and migration [1]. Indeed, NO donors, transfection of eNOS gene into the arterial wall and supplementation of diet with L-arginine have been shown to reduce intimal hyperplasia, a hallmark of atherosclerotic disease [8,9]. However, contrary to these findings, NO has also been implicated in endothelial cell proliferation in conditions where no exogenous physical or chemical stimulus is exerted on cells [3,10].

In recent years, reactive oxygen species (ROS), produced in particular by NAD(P)H oxidase, have been associated with the bioavailability of NO in cardiovascular system. NAD(P)H oxidase is predominantly expressed in phagocytic cells and plays a vital role in non-specific host defense by generating excess amounts of superoxide anion (O_2^-) during

so-called respiratory burst [11]. The membrane-bound components of (p22-phox and gp91-phox that make up cytochrome b_{558} which is responsible for enzyme activity and stability as a whole) a phagocyte-like NAD(P)H oxidase have also been characterized in endothelial cells [12]. Although low level production of ROS in non-phagocytic cells seems to be beneficial and is involved in several regulatory cellular processes including gene expression, higher quantities of ROS are implicated in the pathogenesis of atherosclerosis through activating VSMC proliferation and migration [1,13,14]. It is well-documented that endothelial ROS production increases by several stimuli including pulsatile stretch, hypoxia-reoxygenation and phorbol esters [15-17]. However, the precise role of NAD(P)H oxidase in endothelial cell growth remains to be determined.

In light of these findings, the present study was designed firstly to investigate the relationship between the state of cell growth and concurrent expression and activity of eNOS and NAD(P)H oxidase enzymes using proliferating versus confluent rat CMEC; secondly to assess the effects of enhanced or diminished availability of NO and O_2^- on CMEC growth; and finally to determine the putative molecular mechanism(s) that may be involved in NO- and/or O_2^-- mediated coronary endothelial cell growth.

2. Materials and Methods

The investigation conforms to the "*Guide for the Care and Use of Laboratory Animals*" published by the US National Institutes of Health (NIH Publication No. 85-23, revised 1996).

2.1. Isolation and culture of rat CMEC

CMEC were isolated from 12-14 week-old Sprague Dawley rats using a retrograde constant-flow Langendorff system. Briefly, the hearts were mounted and perfused with 0.04% collagenase for 30 min prior to dissection of the ventricles from the hearts and quenching of collagenase with bovine serum albumin. CMEC were obtained by

sedimentation of myocytes and incubated in 0.01% trypsin at 37°C to prevent non-endothelial cell attachment. Cells were then activated by washing twice in Ca^{2+} (250 and 500 μM) and suspended in Medium 199 supplemented with L-glutamine, sera and antibiotic/antifungal agents. Cell suspensions were plated and incubated at 37°C under 5% CO_2. After 1 h incubation, unattached cells were washed off with saline and remaining cells were cultured to confluence.

Cells were characterized as endothelial by their typical "cobblestone" morphology and their ability to form capillary-like tubes on the Matrigel [18].

2.2. Manipulation of cell growth

To exclude potential effects produced by differences in cell density e.g. cell contact, an identical number of cells was seeded into flasks (0.5×10^6) after the first passage. Cell passages were performed using a 1:3 ratio and culture medium was replaced every 24 h. This ensured that the number of mitoses required to obtain a given degree of confluence (50 and 100%) was unaltered amongst experiments. Cells were not studied post-confluence due to evident contact inhibition in CMEC. Level of confluence was determined by visual inspection every 24 h and by determining the quantities of total protein in each flask using the Lowry method at the end of experiments (Bio-Rad).

2.3. Analysis of mRNA expressions by Northern blotting

Total RNA was extracted using guanidinium thiocyanate-phenol-chloroform extraction method [19]. Equal amounts of total RNA (20 μg), quantified at A_{260} by spectrophotometry, were fractioned on a 1.2% agarose-formaldehyde denaturing gel. The denatured RNA samples were then transferred onto a nylon membrane and ultraviolet cross-linked. The filters were then prehybridized at 42 ^oC for at least 2 h in 5 x SSPE (1 x SSPE: 0.15 M NaCl, 10 mM NaH_2PO_4 and 1 mM EDTA) containing 50% formamide, 5 x Denhardt's solution, 0.4% SDS, and 100 mg/ml salmon sperm DNA. Hybridizations

were performed overnight with [^{32}P]-dCTP-random-prime-labeled eNOS or GAPDH cDNA probes that were prepared as previously described [20]. The filters were then washed to a final stringency of 0.1 x SSPE / 0.1% SDS at 65 ^{o}C and exposed to KODAK X-100 XAR film (Sigma) with intensifying screens at -80 ^{o}C. Quantification of autoradiograms was performed by densitometry, and values for eNOS were normalized to those of GAPDH.

2.4. Analysis of protein expression by Western blotting

Cells were washed twice in ice-cold PBS prior to lysis in boiling lysis solution containing 1% SDS and 10 mM Tris pH 7.4. The insoluble material was removed by centrifugation and protein concentration in the supernatant was measured by the Lowry method (Bio-Rad). Equal amounts of protein were run on 8% SDS-polyacrylamide gels and electroblotted onto nitrocellulose membrane (Hybond N^{+}, Amersham Pharmacia). Equal rate of transfer among lanes was confirmed by reversible staining with Ponceau S (Sigma). The membrane was then incubated with a primary antibody specific for either eNOS (BD Transduction Labs.) or p22-phox (a kind gift of Dr MT Quinn, Bozeman, USA) protein. Horseradish peroxidase-linked secondary antibodies were used and the immunocomplex was developed using an ECL Plus detection kit (Amersham Pharmacia) and exposed to KODAK X-100 XAR film (Sigma). The autoradiographs were analyzed by scanning densitometry with subtraction of the background counts measured outside loaded lanes.

2.5. Measurement of NOS activity

NOS activity was measured by the conversion of L-[^{3}H]-arginine to L-[^{3}H]-citrulline. Briefly, CMEC were homogenized, on ice, in TRIS buffer (50 mM, pH 7.4) containing leupeptin (0.2 μM), pepstatin A (1.5 mM) and phenylmethylsulfonyl fluoride (PMSF, 1 mM). Samples were incubated at 37 ^{o}C for 30 min in the presence of calmodulin (30 nM),

NADPH (1 mM), H_4B (5 μM), Ca^{2+} (2 mM), L-valine (50 mM) and a mixture of unlabelled (0-5 μM) and L-[^{3}H]-arginine (10 mM) (Amersham Pharmacia). To assess the contribution of iNOS (calcium-independent isoform) to overall NOS activity Ca^{2+} was replaced with EGTA (1 mM). Reactions were terminated by the addition of 1 ml HEPES (20 mM, pH 5.5) containing EDTA (1 mM) and EGTA (1 mM). Newly formed L-[^{3}H]citrulline, neutral at pH 5.5, was separated from the incubation mixture by cation exchange resin (Dowex AG 50 W-X8, Bio-Rad) and quantified using a liquid scintillation counter. Results were expressed as pmol L-citrulline/mg protein/min.

2.6. Nitrite detection

Nitrite levels were measured in cellular homogenates by Griess reaction as an index of NO generation following conversion of nitrate to nitrite by nitrate reductase [21]. An aliquot of the supernatant was mixed with an equal volume of Griess reagent (sulfanilamide 1% w/v, naphthylethylenediamine dihydrochloride 0.1% w/v and orthophosphoric acid 2.5% v/v) and incubated at room temperature for 10 min. The absorbance of the samples was determined at 540 nm wavelength and compared to those of known concentrations of sodium nitrite. The amount of nitrite formed was normalized to the protein content of the respective cell culture flask.

2.7. Measurement of NAD(P)H oxidase activity and detection of O_2^- levels

Cellular homogenates were prepared on ice in lysis buffer containing 1 mM EGTA, 20 mM monobasic potassium phosphate (pH 7.0), 0.5 μM leupeptin, 0.7 μM pepstatin, 10 μM aprotinin and 0.5 mM PMSF. O_2^- levels were measured by lucigenin-enhanced chemiluminescent detection of superoxide in a luminometer. Recently, 5 μM lucigenin has been shown to correlate well with electron spin resonance as a quantitative measurement of O_2^- production [22]. The reaction was initiated by the addition of 200 μg of total protein to reaction buffer containing 1 mM EGTA, 150 mM sucrose, 5 μM

lucigenin and 1 mM NADH or NADPH. Luminescence was calculated as the rate of counts per mg protein after deduction of the counts obtained from a buffer blank [23]. NAD(P)H oxidase activity was measured in similar experiments where the specific inhibitors of other ROS-generating enzymes i.e. L-NAME (0.1 mM), rotenone (50 μM), allopurinol (100 μM) or indomethacin (50μM) were added to cellular homogenates for 60 min before determining O_2^- generation.

O_2^- levels were also measured in additional experiments by cytochrome *C* reduction assays. Briefly, proliferating and confluent CMEC were collected in Hanks' balanced salt solution (HBSS) at a density of 20 x 10^6 cells/ml. Aliquots (250 μl) containing 50 μM cytochrome *C* were then incubated for 60 min at 37 °C. O_2^- generation was measured as the superoxide dismutase (10 μg/ml)-inhibitable reduction of cytochrome *C* and monitored as the change in absorbance at 550 nm using a Cobas-Fara centrifugal analyzer. Absorbances were recorded for 12 min with 90 seconds intervals and production of O_2^- was calculated as pmoles O_2^- per 10^6 cells after subtracting background values measured at 550 nm. NAD(P)H oxidase activity was measured in similar experiments where the aforementioned specific inhibitors of other ROS-generating enzymes i.e. L-NAME (0.1 mM), rotenone (50 μM), allopurinol (100 μM) or indomethacin (50μM) were added to aliquots during 60 min incubation period prior to determining O_2^- generation.

2.8. [^{3}H]Thymidine incorporation

[^{3}H]Thymidine (37 kBq/ml) was directly added to the culture medium with the test compounds and incubated with CMEC for 18 h. Experimental incubations were stopped by removing the medium, washing the cells with ice-cold 5% trichloroacetic acid (TCA) and incubating them in 5% TCA on ice for 20 min. After two additional washings with cold 95% ethanol, precipitates were solubilized with buffer (0.1 M NaOH, 2% Na_2CO_3,

1% sodium dodecyl sulfate) and their radioactivity was analyzed by liquid scintillation counting. Data are expressed as cpm [^{3}H]thymidine incorporated per flask.

2.9. Evaluation of Cell Viability

In order to detect cytotoxicity of aforementioned treatments on CMEC, a small aliquot of cells following incubation with any of the agents was incubated in 0.1% trypan blue for a few minutes and viewed under a light microscope. Dead cells were permeable to trypan blue and thus become colored. By counting 100 cells, the percentage of viable cells was calculated.

2.10. CMEC Transfection

The full-length rat endothelial cell p22-phox cDNA was generated using the primers and experimental conditions as previously described [15]. The PCR product was sequenced and cloned in sense and antisense orientations into the expression vector pcDNA 3.1 (Invitrogen). Inserted cDNA orientations were determined using a differential digest. CMEC were transfected with pcDNA 3.1 containing the sense, antisense or the empty vector as a control using Lipofectamine Plus reagent (Gibco BRL). CMEC were trypsinized on the day before transfection and seeded to obtain a density of 2 x 10^6 cells/T25 flasks. The following day 5 μg of plasmid DNA was mixed with 300 μl of serum-free DMEM in a sterile eppendorf tube prior to addition of 50 μl of transfection agent. The mixture was incubated at room temperature for 15 min before combining with 3 ml of DMEM containing 20% fetal bovine serum, 500 U/ml penicillin and 50 μg/ml streptomycin (all from Gibco BRL) and washing with PBS before plating into T25 flasks. The cells were incubated for 3 h at 37 ^oC in 95% air/5%CO_2. The transfected cells were then washed twice with PBS and allowed to recover overnight. The following day, the medium was replaced with appropriate culture medium and cells were cultured for a further 3 days before harvesting.

2.11. Immunocytochemistry

CMECs grown on coverslips were rinsed with ice-cold PBS and fixed in 3.7% formaldehyde for 15 min at room temperature before permeabilization with 0.1% Triton X-100. Coverslips were washed and incubated with 20% fetal calf serum in PBS (pH 7.4) prior to incubation with an anti-p22-phox primary antibody (monoclonal antibody 449, a kind gift Dr A. Verhoeven, Central Laboratory of Blood Transfusion, Amsterdam, The Netherlands) in PBS with 0.1% BSA and 0.01% NaN_3. The primary antibody staining was visualized with FITC-conjugated goat anti-mouse antibody (1:200 dilution, Sigma). Normal mouse IgG (5 μg/ml) was used instead of primary antibody as negative controls. The cells were then examined using a Zeiss Axiovert fluoresecence microscope and photographs were taken on Ilford Hp5 Plus film (ASA 400) uprated to ASA1600 during development.

2.12. Statistical analysis

Data are expressed as mean ± SEM. Student's *t-test* was used for the comparison of data. *P* values less than 0.05 were considered to be statistically significant.

3. Results

3.1. Effect of cell growth on eNOS and p22-phox mRNA and protein expressions

Northern blot analyses detected a single expected size transcript, namely, 4.3 kb (eNOS), 0.8 kb (p22-phox) and 1.8 kb (GAPDH), for each gene of interest (Fig. 1A). The densitometric analysis of autoradiograms revealed an approximately 3-fold increase in mRNA expressions of both eNOS and p22-phox in proliferating versus resting CMEC after normalizing to GAPDH mRNA levels (Fig. 1B).

Since the alterations in mRNA levels may not necessarily reflect the changes in corresponding proteins, the levels of protein expression were investigated by Western analyses which revealed expected size products for both eNOS (140 kDa) and p22-phox

(~22 kDa) (Fig. 2A). Analyses of the Western autoradiograms showed 3.5- and 2.5-fold increases in eNOS and p22-phox protein levels in 50% versus 100% confluent CMEC after normalizing to α-tubulin protein levels (Fig. 2B).

3.2. Effect of cell growth on NO and O_2^- generation

Cell density in 50% and 100% confluent flasks was determined by measurement of total cellular protein which revealed 331 ± 21 μg and 606 ± 53 μg at 50 and 100% confluence, respectively (n=5, $P< 0.05$). The relative changes in protein levels were reflective of the number of cells as counted after trypsinization from matching randomly chosen flasks ($1.01 \pm 0.23 \times 10^6$ vs $2.15 \pm 0.39 \times 10^6$, n=5, $P< 0.05$).

The levels of both O_2^- and nitrite, measured as an index of NO generation, were found to be significantly higher in proliferating versus confluent CMEC (Fig. 3A-B). Similar increases were also observed in both NAD(P)H oxidase activity and eNOS activity as measured by cytochrome *C* reduction and L-[^{3}H]-arginine to L-[^{3}H]-citrulline conversion assays, respectively (Fig 3C-D). However, no difference was observed in iNOS activity between proliferating and resting CMEC (0.084 ± 0.01 vs 0.079 ± 0.01 pmol L-citrulline/mg protein/min, n=5, $P> 0.05$).

3.3. Effect of NO and O_2^- on cell growth

To determine the effects of exogenous NO on CMEC proliferation, the cells were incubated for 24 h with spermine NONOate (SpNO, 0.1-1 μM). SpNO was prepared in phosphate buffered saline (pH 8.5) to release NO at a predictable rate that does not require bioconversion to NO [24]. The incubation with SpNO almost completely abolished CMEC proliferation in proliferating cells as determined by the levels of total cellular protein (331 ± 21 μg vs 357 ± 23 μg. n=5, $P> 0.05$), by cell counting ($1.01 \pm 0.23 \times 10^6$ vs $1.14 \pm 0.16 \times 10^6$, n=5, $P> 0.05$) and by the measurement of [^{3}H]thymidine incorporation in treatment versus control flasks (Fig. 4). SpNO had similar effects on total

cellular protein levels (606 ± 53 μg vs 648 ± 59 μg. n=5, *P*> 0.05), cell number (2.15 ± 0.39 x 10^6 vs 2.46 ± 0.29 x 10^6, n=5, *P*> 0.05) and [^{3}H]thymidine incorporation rates of confluent CMEC (data not shown).

In contrast, the incubation of proliferating CMEC with a O_2^--generator, pyrogallol (50-150 μM), for 24 h produced a dramatic increase in cell number (1.01 ± 0.23 x 10^6 vs 1.76 ± 0.28 x 10^6, n=5, *P*< 0.05), in total cellular protein levels (331 ± 21 μg vs 448 ± 37μg. n=5, *P*< 0.05) and in the rates of [^{3}H]thymidine incorporation after treatment (Fig. 4). However, pyrogallol treatment did not alter either cell number (2.15 ± 0.39 x 10^6 vs 2.28 ± 0.41 x 10^6, n=5, *P*> 0.05), total protein levels (606 ± 53 μg vs 633 ± 41 μg. n=5, *P*> 0.05) or [^{3}H]thymidine incorporation in confluent CMEC (data not shown).

3.5. Effect of peroxynitrite on [^{3}H]thymidine incorporation in CMEC

The experiments thus far demonstrated a direct correlation between cell proliferation and the number of cells, their total protein content and [^{3}H]thymidine incorporation. To determine whether peroxynitrite, formed by the reaction between NO and O_2^-, affects [^{3}H]thymidine incorporation and hence cell proliferation, CMEC were treated with pyrogallol (150 μM) or SpNO (1 μM) in the presence of a cell permeable superoxide dismutase (SOD) mimetic, MnTBAP (200 U/ml). Neither treatment significantly altered the rate of DNA synthesis compared to solely pyrogallol- or SpNO-treated CMEC (Fig.5).

3.6. Effect of eNOS and NAD(P)H oxidase inhibitors on cell growth

The incubation of proliferating CMEC with L-NAME (50 and 250 μM), a NOS inhibitor, for 24 h significantly enhanced the level of [^{3}H]thymidine incorporation compared to untreated control groups. However, the treatment of proliferating CMEC with two structurally-different inhibitors of NAD(P)H oxidase, namely apocynin (0.3 and 3 mM) and diphenyleneiodinium (DPI, 1 and 10 μM) markedly diminished cell growth in

a dose-dependent manner as determined by the measurements of [^{3}H]thymidine incorporation (Fig. 6A). The inhibitors of other O_2^--generating enzymes, including xanthine oxidase (allopurinol, 10-100 μM), cyclooxygenase (indomethacin, 10-100 μM) and mitochondrial NAD(P)H oxidase (rotenone, 10-100 μM) did not alter cell growth as assessed by [^{3}H]thymidine incorporation (Fig. 6B).

3.7. Effect of p22-phox sense and antisense cDNA transfection on CMEC growth

Transfection of CMECs at an efficiency of 13 ± 2 % with antisense p22-phox cDNA resulted in a substantial reduction in p22-phox protein expression as assessed by Western analyses and immunocytochemistry experiments whereas transfection with sense p22-phox cDNA or empty vector had no effect on these parameters (Fig. 7A-B). Transfection with antisense p22-phox also markedly diminished NAD(P)H oxidase activity, without affecting the cell viability as analyzed by trypan blue exclusion assay, compared to untreated cells and CMEC transfected with either empty vector or sense p22-phox cDNA (Fig. 8A). Similarly, three days after transfection the number of CMECs transfected with antisense p22-phox cDNA were, by approximately 30%, lesser compared to CMEC transfected with empty vector or sense p22-phox cDNA. These data were in good agreement with our findings showing a similar degree of decrease in [^{3}H]thymidine incorporation rate in CMEC transfected with antisense p22-phox cDNA but not with empty vector or sense p22-phox cDNA (Fig. 8B).

4. Discussion

The vascular endothelium, composed of a layer of endothelial cells, has recently been established as a strategically-located organ that can generate a wide selection of components to modulate vascular tone through regulating the functions of underlying VSMC in response to several chemical, physical or hormonal stimuli [1]. The integrity of the endothelium therefore bears an enormous significance in physiological processes -

e.g. wound healing after an injury to the vascular wall - where controlled proliferation and migration of endothelial cells are required [2]. However, several pathological conditions including coronary atherosclerosis, a major cause of morbidity and mortality in the Western World, are associated with an uncontrolled as well as accelerated proliferation and migration of both endothelial and VSMCs [5].

It is well-documented that NO, generated by eNOS, inhibits proliferation of a number of cell types including VSMC and lymphocytes thus prevents the initiation and/or progression of atherosclerotic disease [25,26]. It is also well-known that ROS, produced by NAD(P)H oxidase, determine bioavailability of NO in the cardiovascular system and are implicated in the pathogenesis of atherosclerosis through their ability to enhance VSMC proliferation and migration [13,14]. However, the current data as to the effects of NO on endothelial cell growth are rather contradictory in that both growth-stimulating [3,10] and growth-inhibiting effects have been reported [27-29]. Besides, the effects of endothelial cell growth on the activity and expression of NAD(P)H oxidase remains to be fully elucidated, although the correlation between cell growth and enzymatic regulation of eNOS has recently been well-documented [20]. The present study was therefore designed to investigate the reciprocal relationship between coronary endothelial cell growth and the concurrent expression and activity of the enzymes, namely, eNOS and NAD(P)H oxidase that are associated with the regulation of endothelial cell redox state. All the experiments outlined in the current study were carried out using early-passage cultured rat CMEC in order to avoid the effects of changes in coronary endothelial cell phenotype on enzyme expression and activity [30]. Significant increases in eNOS mRNA and protein expressions, eNOS activity and consequently in nitrite generation, the ultimate breakdown product of NO, were observed in proliferating versus confluent CMEC. Similar increases in these parameters have recently been reported in rat CMEC and aortic

endothelial cells in which the effects of angiotensin II on NO production and eNOS mRNA/protein expressions were investigated in relation to the state of cell growth [20,31]. However, in the current study no marked difference was observed in iNOS activity between growing and quiescent rat CMEC in contrast to elevation in eNOS activity. This result confirms that eNOS serves as the endogenous source of NO during coronary endothelial cell growth under conditions where no external stimulus like shear stress, cyclic strain or hyperglycemia is imposed on cells.

In order to determine the reciprocal effect of NO on CMEC growth and indeed to ensure whether endogenously-produced and exogenously-added NO elicit different effects on cell growth, the CMEC were treated with a NOS inhibitor, L-NAME or a NO donor, SpNO. The former treatment led to a significant increase in cell growth while the latter dramatically inhibited proliferation as assessed by three different experimental procedures, namely, cell counting and by measurements of total cellular proteins and [^{3}H]thymidine incorporation rates. Taken together, these data suggest that endothelial cells produce physiologically relevant concentrations of NO to preserve the integrity of endothelium and perhaps vascular wall as a whole. However, once the adequate synthesis of endogenous NO is attenuated, in this case via inactivation of NOS, the intracellular oxidative balance may tilt in favor of ROS that in turn accelerate endothelial cell proliferation. On the contrary, the exogenous supplementation of NO via NO-donors at higher concentrations that is normally associated with disease conditions like sepsis and inflammation generates a pool of NO that cannot be neutralized by O_2^- and therefore results in the suppression of cell proliferation. In support of our results and hypothesis, a previous study has also shown that NO-generating compounds namely, S-nitroso-acetylpenicillamine (SNAP), sodium nitroprusside (SNP) and S-nitroso-glutathione (GSNO) inhibit human umbilical vein EC and human coronary artery EC proliferation

[32]. The inhibitory effects of NO on cell proliferation and migration has also been shown in a number of other cell lines such as fibroblasts, mesangial cells and VSMCs thereby proving that its suppressive effects are not specific to endothelial cells [27-29,33,34].

The present study has shown that CMEC growth also regulates NAD(P)H oxidase activity and O_2^- generation, a process that may be critical in normalization of enhanced NO levels. Indeed, increases in overall NAD(P)H oxidase activity and O_2^- production as well as mRNA and protein expressions of p22-phox, a membrane-bound component of NAD(P)H oxidase system, have been demonstrated in proliferating compared to resting CMEC. NAD(P)H oxidase is a multicomponent enzyme system that consists of several cytsosolic subunits including p47-phox and p67-phox as well as two membrane-bound components namely p22-phox and gp91-phox that make up cytochrome b_{558} [11,12]. Since cytochrome b_{558} accounts for enzyme activity and stability as a whole, it is assumed that the alteration(s) occur in the expression of one subunit is/are reflective of similar changes in the other [12]. Hence, the current study solely concentrated on the changes in mRNA and protein expression of p22-phox subunit that is expressed in abundance in CMEC [12].

The correlation between CMEC growth and O_2^- bioavailability was further investigated in additional experiments in that cells were treated with either one of the two structurally unrelated inhibitors of NAD(P)H oxidase enzyme, namely DPI or apocynin or a O_2^--generator i.e. pyrogallol. Both inhibitors significantly abrogated CMEC growth in a dose-dependent fashion while pyrogallol significantly induced cell proliferation in 50% but not in 100% confluent CMEC. Similarly, transfection of CMEC with antisense p22-phox cDNA that resulted in a substantial reduction in p22-phox protein expression and NAD(P)H oxidase activity also significantly reduced CMEC proliferation and [^{3}H]thymidine incorporation without affecting overall cell viability. In contrast,

transfection of CMEC with sense p22-phox cDNA or empty vector had no effect on these parameters. It is noteworthy in this context that, the inhibitors of xanthine oxidase, cyclooxygenase and mitochondrial NAD(P)H oxidase did not affect CMEC growth. These results were in agreement with a previous study using three different human endothelial cell lines and showing ROS derived from NAD(P)H oxidase but not eNOS or xanthine oxidase as critical elements in endothelial cell growth [35].

The reaction between NO and O_2^- generates $OONO^-$ at a rate of 6.7×10^9 ms^{-1} and this rate is three times faster than the reaction between O_2^- and SOD [36,37]. The formation of $OONO^-$ is a double-edged sword; on one hand potentially deleterious O_2^- is neutralized, on the other hand the most potent vasodilator NO is consumed in the process. Hence, $OONO^-$ has been proposed as a toxic compound causing tissue damage, lipid peroxidation or as a protective molecule improving cellular vitality and relaxation of VSMC [38,39]. The involvement of $OONO^-$ in CMEC proliferation or its inhibition was therefore rather important. In the current study the proliferating CMEC were treated with SpNO or pyrogallol alone or in the presence of a cell-permeable SOD mimetic, MnTBAP. It has been demonstrated that the addition of SOD did not interfere with the effects of NO or O_2^- *per se* thereby indicating that NO donors and pyrogallol mediate their effects by releasing NO and O_2^-, respectively.

The elucidation of the regulatory effects of endothelial cell growth on eNOS and NAD(P)H oxidase expression and activities may have significant implications in the pathogenesis of atherosclerosis in that proliferation and migration of VSMCs contribute to formation of atheroma. Since NO inhibits these effects, enhanced NO production by proliferating CMEC may attenuate the development of coronary artherosclerosis. In contrast, activation of NAD(P)H oxidase enzyme and therefore generation of excess quantities of O_2^- in the same cells may diminish the beneficial effects of NO and

accelerate disease formation. These findings imply that EC growth is tightly coupled to the redox state of the cell and suppression of NAD(P)H oxidase activity may provide a foundation for the therapy of atherosclerotic disease.

Acknowledgements

This study was in part supported by the grants to Dr Bayraktutan from the Royal Society UK and Northern Ireland Chest Heart & Stroke Association.

References

1. Bayraktutan, U. Free radicals, diabetes and endothelial dysfunction. Diabet Obes Metabol 2002; 4: 224-238.
2. Lee PC, Salyapongse AN, Bragdon GA, Shears LL, Watkins SC, Edington HD, Billiar TR. Impaired wound healing and angiogenesis in eNOS-deficient mice. Am J Physiol 1999; 277: H1600-1608.
3. Ziche M, Morbidelli L, Masini E, Amerini S, Granger HJ, Maggi CA, et al. Nitric oxide mediates angiogenesis in vivo and endothelial cell growth and migration in vitro promoted by substance P. J Clin Invest 1994; 94: 2036-2044.
4. Vacca A, Bruno M, Boccarelli A, Coluccia M, Ribatti D, Bergamo A, et al. Inhibition of endothelial cell functions and of angiogenesis by the metastasis inhibitor NAMI-A. Br J Cancer 2002; 86: 993-998.
5. Werba JP, Martinez V, Abulafia DP, Levy R, Magarinos G, Rey RH, et al. Marked neointimal lipoprotein lipase increase in distinct models of proclivity to atherosclerosis: a feature independent of endothelial layer integrity. Atherosclerosis 2001; 156: 91-101.
6. Ranjan V, Xiao Z, Diamond SL. Constitutive NOS expression in cultured endothelial cells is elevated by fluid shear stress. Am J Physiol 1995; 269: H550-H555.

7. McQuillan LP, Leung GK, Marsden PA, Kostyk SK, Kourembanas S. Hypoxia inhibits expression of eNOS via transcriptional and posttranscriptional mechanisms. Am J Physiol 1994; 267: H1921-H1927.
8. Kojda G, Noack, E. Effects of pentaerythrityl-tetranitrate and isosorbide-5-mononitrate in experimental atherosclerosis. Agents Actions Suppl 1995; 45: 201-206.
9. von der Leyen HE, Gibbons GH, Morishita R, Lewis NP, Zhang L, Nakajima M, et al. Gene therapy inhibiting neointimal vascular lesion: in vivo transfer of eNOS gene. Proc Natl Acad Sci USA 1995; 92: 1137-1141.
10. Morbidelli L, Chang CH, Douglas JG, Granger HJ, Ledda F, Ziche M. Nitric oxide mediates mitogenic effect of VEGF on coronary venular endothelium. Am J Physiol 1996; 270: H411-H415
11. Thrasher AJ, Keep NH, Wientjes F, Segal AW. Chronic granulomatous disease. Biochim Biophys Acta 1994; 1227: 1-24.
12. Bayraktutan U, Blayney L, Shah AM. Molecular characterisation and localisation of the NAD(P)H oxidase components gp91-phox and p22-phox in endothelial cells. Arterioscler Thromb Vasc Biol 2000; 20: 1903-1911.
13. Li PF, Dietz R, von Harsdorf R. Differential effect of hydrogen peroxide and superoxide anion on apoptosis and proliferation of vascular smooth muscle cells. Circulation 1997; 96: 3602-3609.
14. Lee SL, Wang WW, Fanburg BL. Superoxide as an intermediate signal for serotonin-induced mitogenesis. Free Radic Biol Med 1998; 24: 855-888.
15. Kim KS, Takeda K, Sethi R, Pacyk JB, Tanaka K, Zhou YF, et al. Protection from reoxygenation injury by inhibition of rac1. J Clin Invest 1998; 101: 1821-1826.

16. De Keulenaer GW, Chappell DC, Ishizaka N, Nerem RM., Alexander RW, Griendling KK. Oscillatory and steady laminar shear stress differentially affect human endothelial cell redox state: role of a superoxide-producing NADH oxidase. Circ Res 1998; 82: 1094-1101.
17. Matsubara T, Ziff M. Increased superoxide anion release from human endothelial cells in response to cytokines. J Immunol 1986; 137: 3295-3298.
18. Nishida M, Carley WW, Gerritsen ME, Ellingsen O, Kelly RA. Isolation and characterization of human and rat cardiac microvascular endothelial cells. Am J Physiol 1993; 264: H639-H652.
19. Chomczynski P, Sacchi N. Single-step method of RNA isolation by acid guanidinium thiocyanate-phenol-chloroform extraction. Anal Biochem 1987; 162: 156-159.
20. Bayraktutan U, Ulker S. Effects of ang II on nitric oxide generation in proliferating and quiescent rat coronary microvascular endothelial cells. Hypertens Res 2003; 26: 749-757.
21. Green LC, Wagner DA, Glogowski J, Skipper PL, Wishnok JS, Tannenbaum SR. Analysis of nitrate, nitrite and [^{15}N]nitrate in biological fluids. Anal Biochem 1982; 126: 131-138.
22. Li Y, Zhu H, Kuppusamy P. Validation of lucigenin as a chemiluminogenic probe for detecting superoxide anion radical production by enzymatic and cellular systems. J Biol Chem 1998; 273: 2015-2023.
23. Griendling KK, Minieri CA, Ollerenshaw JD, Wayne AR. Angiotensin II stimulates NADH and NADPH oxidase activity in cultured vascular smooth muscle cells. Circ Res 1994; 74: 1141-1148.

24. Maragos CM, Morley DA, Wink TM, Dunams JE, Keefer LK. Complexes of NO with nucleophiles as agents for the controlled biological release of nitric oxide: vasorelaxant effects. J Med Chem 1991; 34: 3242-3247.
25. Kosonen O, Kankanranta H, Vuorinen P, Moilanen E. Inhibition of lymphocyte proliferation by nitric oxide-releasing oxatriazole derivatives. Eur J Pharmacol 1997; 337: 55-61.
26. Dubey RK, Overbeck HW. Culture of rat mesenteric arteriolar smooth muscle cells: effects of platelet –derived growth factor, angiotensin and nitric oxide on growth. Cell Tissue Res 1994; 275: 133-141.
27. Sarkar R, Webb RC, Stanley JC. Nitric oxide inhibition of endothelial cell mitogenesis and proliferation. Surgery 1995; 118: 274-279.
28. Raychaudhury A, Frischer H, Malik AB. Inhibition of endothelial cell proliferation and bGFG-induced phenotypic modulation by nitric oxide. J Cell Biochem 1996; 63: 125-134.
29. Lopez-Farre A, de Miguel LS, Caramelo C, Gomez-Macias J, Garcia R, Mosquera JR, et al. Role of nitric oxide in autocrine control of growth and apoptosis of endothelial cells. Am J Physiol 1997; 272: H760-H768.
30. Lang D, Bell JP, Bayraktutan U, Small GR, Shah AM, Lewis MJ. Phenotypic changes in rat and guinea pig coronary microvascular endothelium after culture: loss of NO synthase activity. Cardiovsc Res 1999; 42: 794-804.
31. Bayraktutan U. Effects of ang II on nitric oxide generation in growing and resting rat aortic endothelial cells. J Hypertens 2003; 21: (in press)
32. Heller R, Polack T, Grabner R, Till U. Nitric oxide inhibits proliferation of human endothelial cells via a mechanism independent of cGMP. Atheroscler 1999; 144**:** 49-57.

33. Garg UC, Hassid A. Nitric oxide-generating vasodilators and 8-bromo-cyclic guanosine monophosphate inhibit mitogenesis and proliferation of cultured rat VSMCs. J Clin Invest 1989; 83: 1774-1777.
34. Garg UC, Hassid A. NO-generating vasodilators inhibit mitogenesis and proliferation of BALB/C 3T3 fibroblasts by a cGMP-independent mechanism. Biochem Biophys Res Commun 1990; 171: 474-479.
35. Abid R, Kachra Z, Spokes KC, Aird WC. NADPH oxidase activity is required for endothelial cell proliferation and migration. FEBS Lett 2000; 486: 252-256.
36. Huie RE, Padmaja S. The reaction of NO with superoxide. Free Radic Res Commun 1993; 18: 195-199.
37. Beckman JS, Koppenol WH. NO, superoxide and peroxynitrite: the good, the bad and the ugly. Am J Physiol 1996; 271: C1424-C1437.
38. Radi R, Beckman JS, Bush KM, Freeman BA. Peroxynitrite-induced membrane lipid peroxidation: The cytotoxic potential of superoxide and NO. Arch Biochem Biophys 1991; 288: 481-487.
39. Mayer B, Schrammel A, Klatt P, Koesling D, Schmidt K. Peroxynitrite-induced accumulation of cGMP in endothelial cells and stimulation of purified soluble guanylyl cyclase. Dependence on glutathione and possible role of S-nitrosylation. J Biol Chem 1995; 270: 17355-17360.

Figure legends

Fig. 1. (A) Representative Northern blots of endothelial nitric oxide synthase (eNOS), p22-phox and GAPDH transcripts amplified from 50 and 100% confluent coronary microvascular endothelial cells (CMEC). (B) Histogram showing the fold increases in eNOS and p22-phox mRNA in 50% versus 100% confluent CMEC, after normalization against GAPDH. Data are expressed as mean ± SEM, n=5, * $P< 0.05$, 50 vs 100% confluent CMEC.

Fig. 2. (A) Representative Western blots showing endothelial nitric oxide synthase (eNOS), p22-phox and α-tubulin protein levels in 50 and 100% confluent coronary microvascular endothelial cells (CMEC). (B) Histogram showing the fold increases in eNOS and p22-phox protein levels in 50% confluent CMEC, after normalization against α-tubulin. Data are expressed as mean ± SEM, n=5, * $P< 0.05$, 50 vs 100% confluent CMEC.

Fig. 3. Effect of varying coronary microvascular endothelial cell (CMEC) confluence on superoxide anion (O_2^-) (A) and nitrite (B) generations and on NAD(P)H oxidase (C) and eNOS activities (D). Data are expressed as mean ± SEM, n=5, * $P< 0.05$, 50 vs 100% confluent CMEC.

Fig. 4. Effects of a NO donor i.e. sepiapterin NO (SpNO) and a superoxide anion-generator, pyrogallol on [^{3}H]thymidine incorporation rates in coronary microvascular endothelial cells (CMEC). Data are expressed as mean ± SEM, n=5, * $P< 0.05$, treated vs untreated CMEC.

Fig. 5. Effects of pyrogallol or SpNO in the absence and presence of a cell permeable superoxide dismutase (SOD) mimetic, MnTBAP (200 U/ml) on [^{3}H]thymidine

incorporation in proliferating coronary microvascular endothelial cells (CMEC). Data are expressed as mean ± SEM, n=5, * $P< 0.05$, treated vs untreated CMEC.

Fig. 6. (A) Effects of different doses of L-NAME, an endothelial nitric oxide synthase (eNOS) inhibitor and two structurally different inhibitors of NAD(P)H oxidase namely, apocynin and diphenyleneiodinium (DPI) on [^{3}H]thymidine incorporation in coronary microvacular endothelial cells (CMEC). (B) Effects of different doses of inhibitors of xanthine oxidase (allopurinol), cyclooxygenase (indomethacine) and mitochondrial NAD(P)H oxidase system (rotenone) on [^{3}H]thymidine incorporation in CMEC. Data are expressed as mean ± SEM, n=5, * $P< 0.05$, treated vs untreated proliferating CMEC.

Fig. 7. (A) Representative Western blots showing p22-phox protein levels in coronary microvascular endothelial cells (CMEC) and in CMEC transfected with sense, empty vector and antisense p22-phox cDNA. (B) Immunofluoresence microscopy showing localization of p22-phox protein in normal CMEC and CMEC transfected with sense, empty vector or antisense p22-phox cDNA.

Fig. 8. (A) Effects of sense, empty vector and antisense p22-phox cDNA transfected coronary microvascular endothelial cells (CMEC) on superoxide anion (O_2^-) generation in comparison with untreated proliferating CMEC. (B) Histogram showing the fold differences in [^{3}H]incorporation in untreated (control) CMEC and CMEC transfected with sense, empty vector and antisense p22-phox cDNA. Data are expressed as mean ± SEM, n=5, * $P< 0.05$, treated vs untreated proliferating CMEC.

A

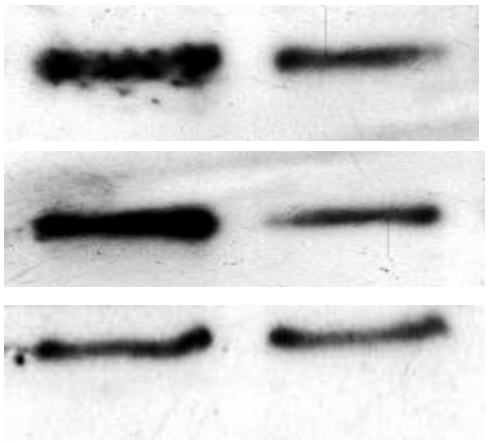
eNOS
p22-phox
GAPDH
50%
100%

B

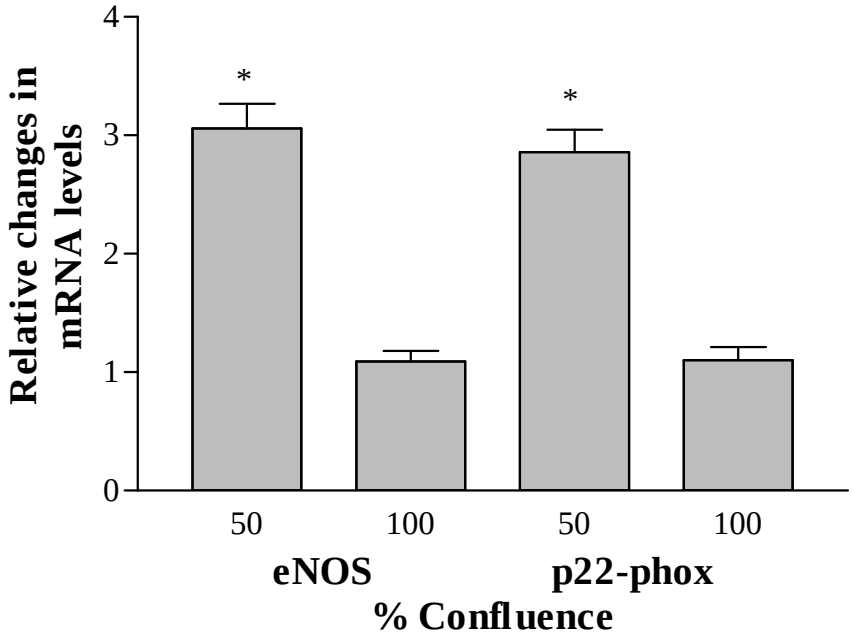
Relative changes in mRNA levels
4
3
2
1
0
*
*
50
100
50
100
eNOS
p22-phox
% Confluence

A

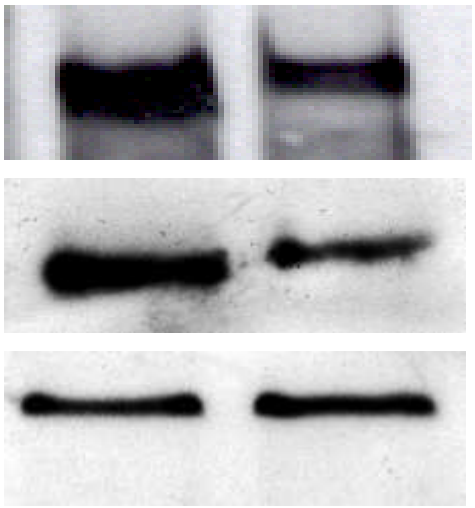
eNOS
p22-phox
α–tubulin
50%
100%

B

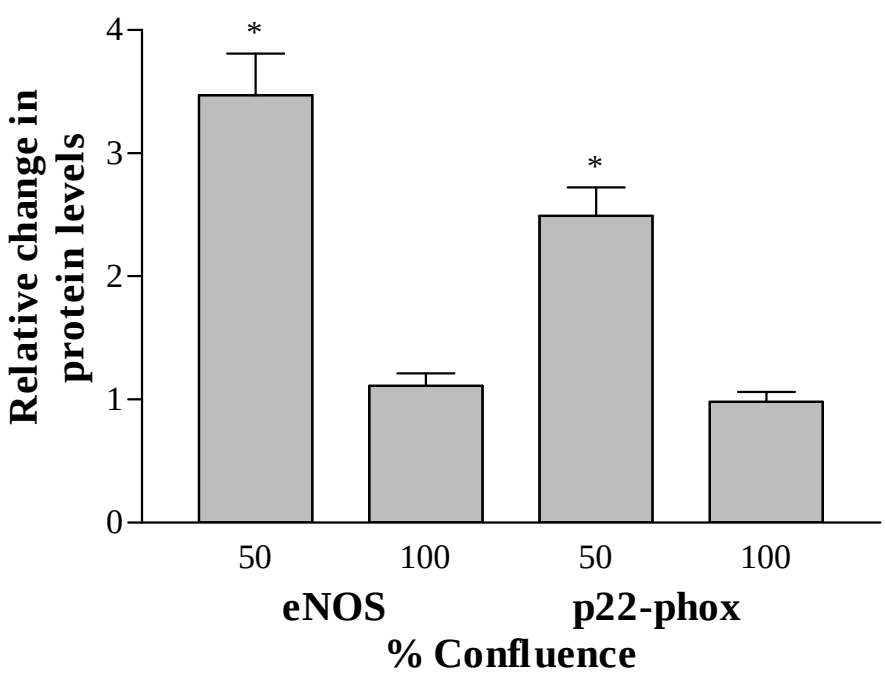
Relative change in protein levels
0
1
2
3
4
*
*
50
100
50
100
eNOS
p22-phox
% Confluence

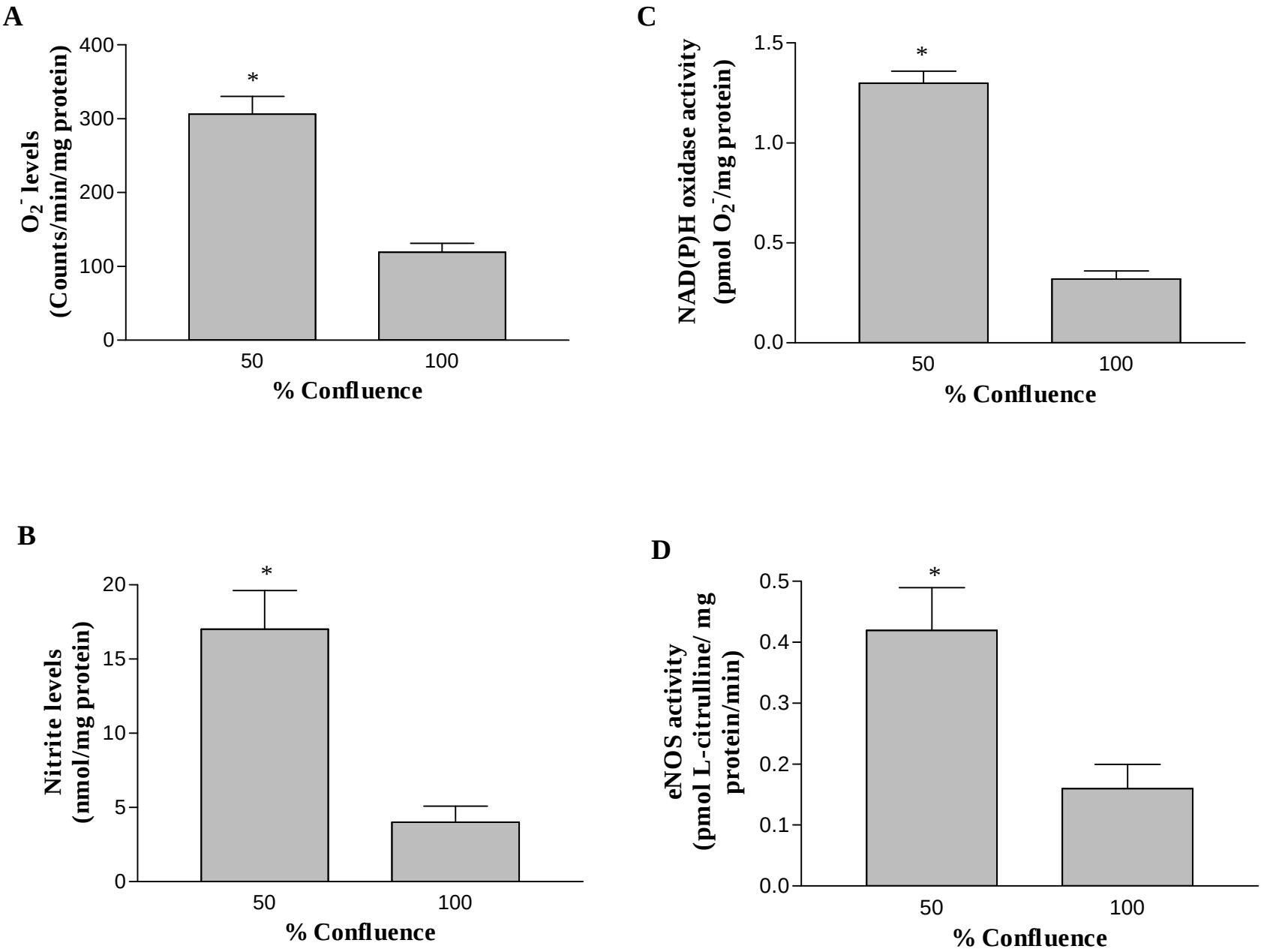
A
O_2^- levels (Counts/min/mg protein)
400
300
200
100
0
*
50
100
% Confluence
C
NAD(P)H oxidase activity (pmol O_2^-/mg protein)
1.5
1.0
0.5
0.0
*
50
100
% Confluence
B
Nitrite levels (nmol/mg protein)
20
15
10
5
0
*
50
100
% Confluence
D
eNOS activity (pmol L-citrulline/ mg protein/min)
0.5
0.4
0.3
0.2
0.1
0.0
*
50
100
% Confluence

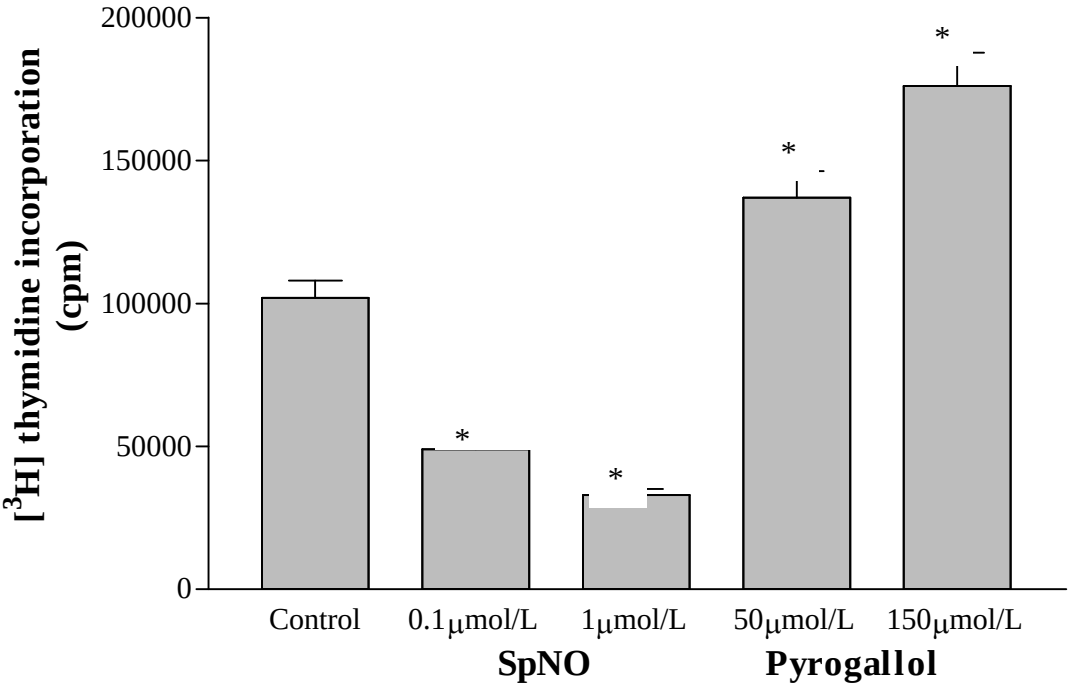
200000
150000
100000
50000
0
[3H] thymidine incorporation (cpm)
*
*
*
*
Control
0.1μmol/L
1μmol/L
50μmol/L
150μmol/L
SpNO
Pyrogallol

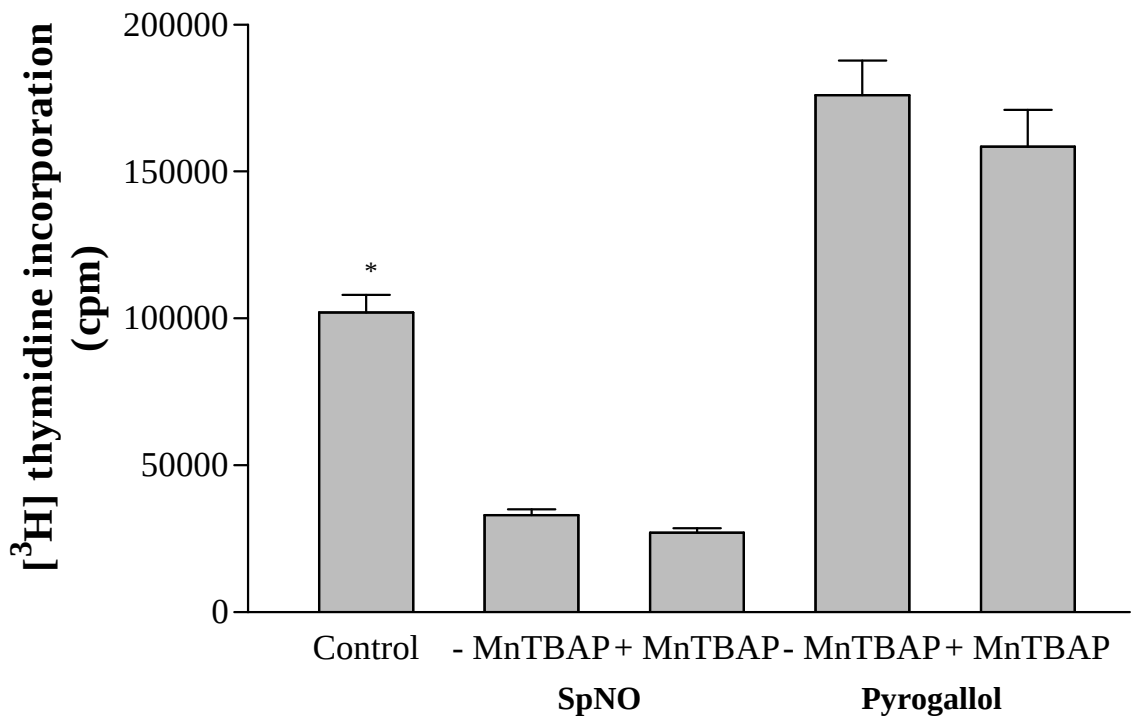
[3H] thymidine incorporation (cpm)
200000
150000
100000
50000
0
*
Control
- MnTBAP
+ MnTBAP
- MnTBAP
+ MnTBAP
SpNO
Pyrogallol

A

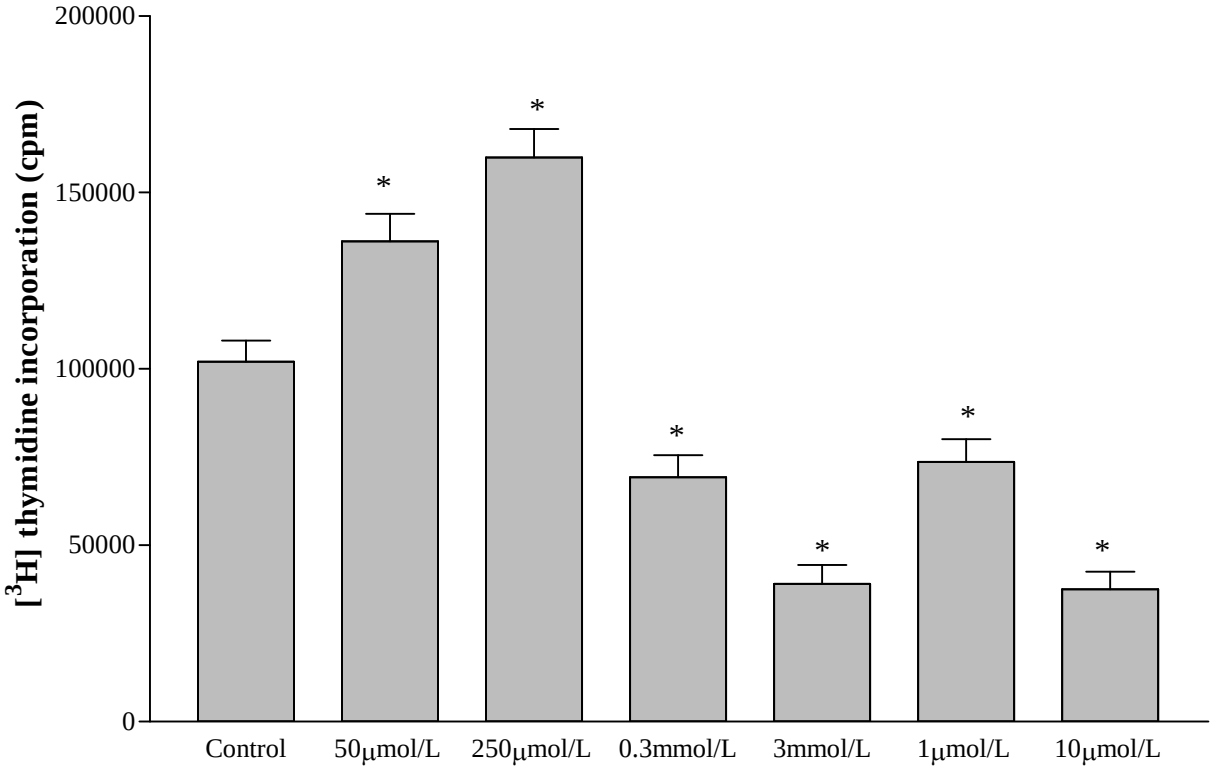
200000
150000
100000
50000
0
[3H] thymidine incorporation (cpm)
*
*
*
*
*
*
Control
50μmol/L
250μmol/L
0.3mmol/L
3mmol/L
1μmol/L
10μmol/L
L-NAME
Apocynin
DPI

B

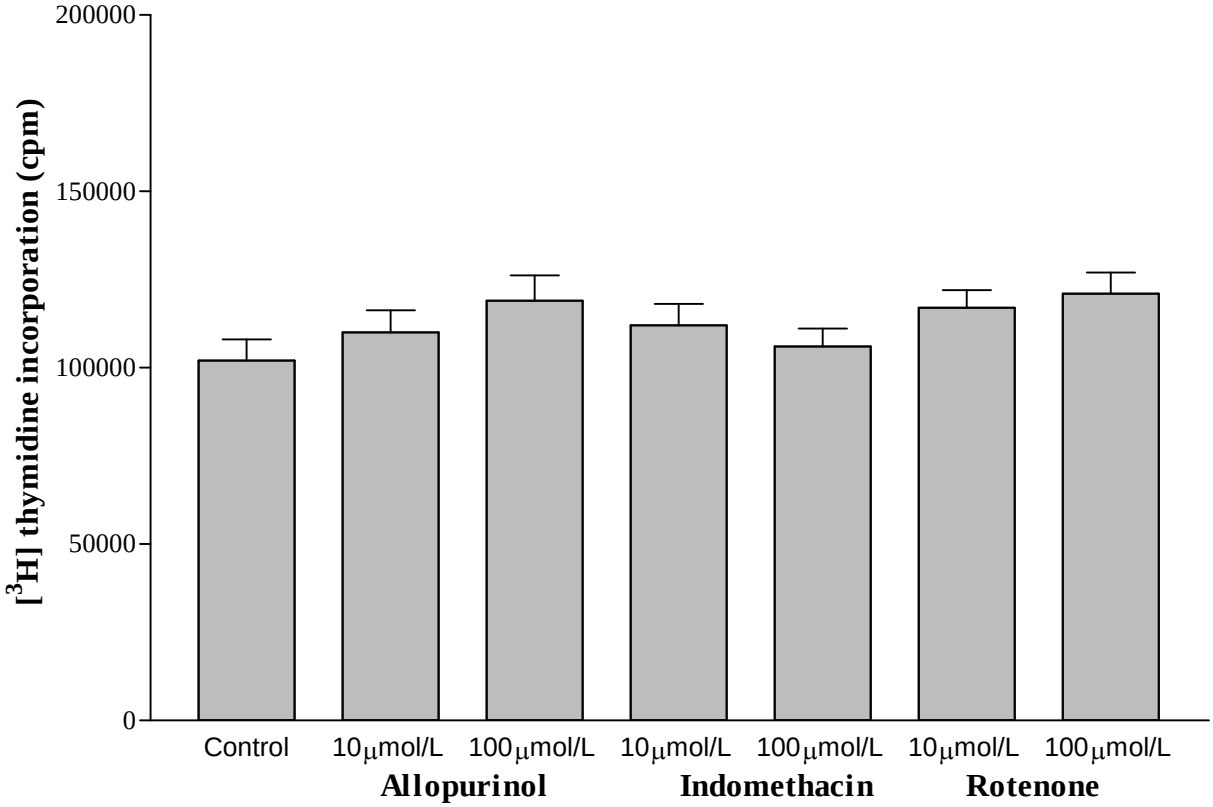
200000
150000
100000
50000
0
[3H] thymidine incorporation (cpm)
Control
10μmol/L
100μmol/L
10μmol/L
100μmol/L
10μmol/L
100μmol/L
Allopurinol
Indomethacin
Rotenone

A

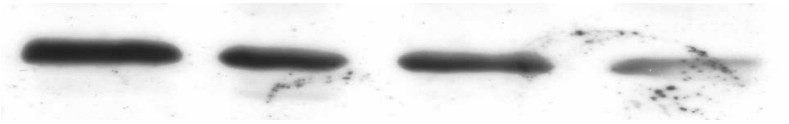

22 kDa

Control **Sense** **Empty vector** **Antisense**

B

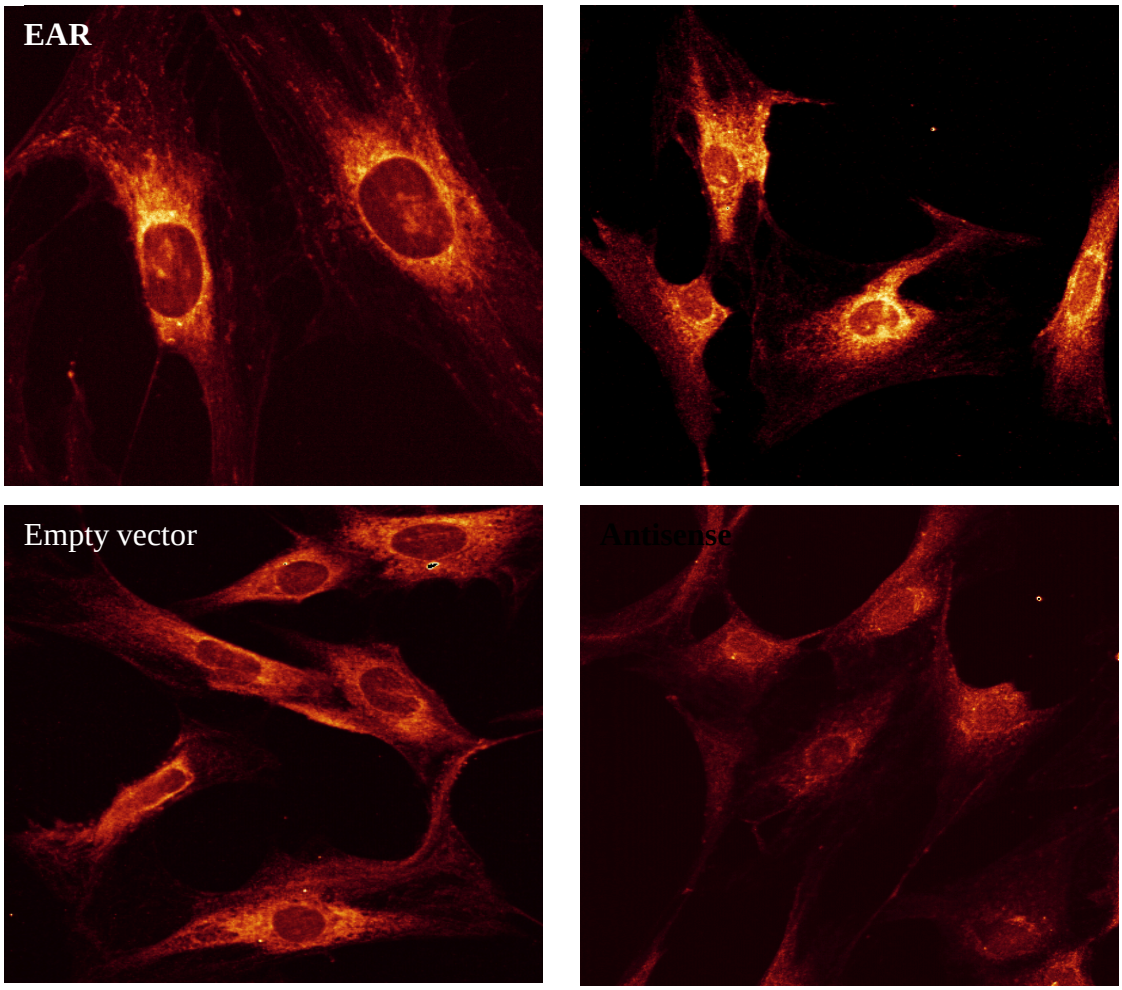

A

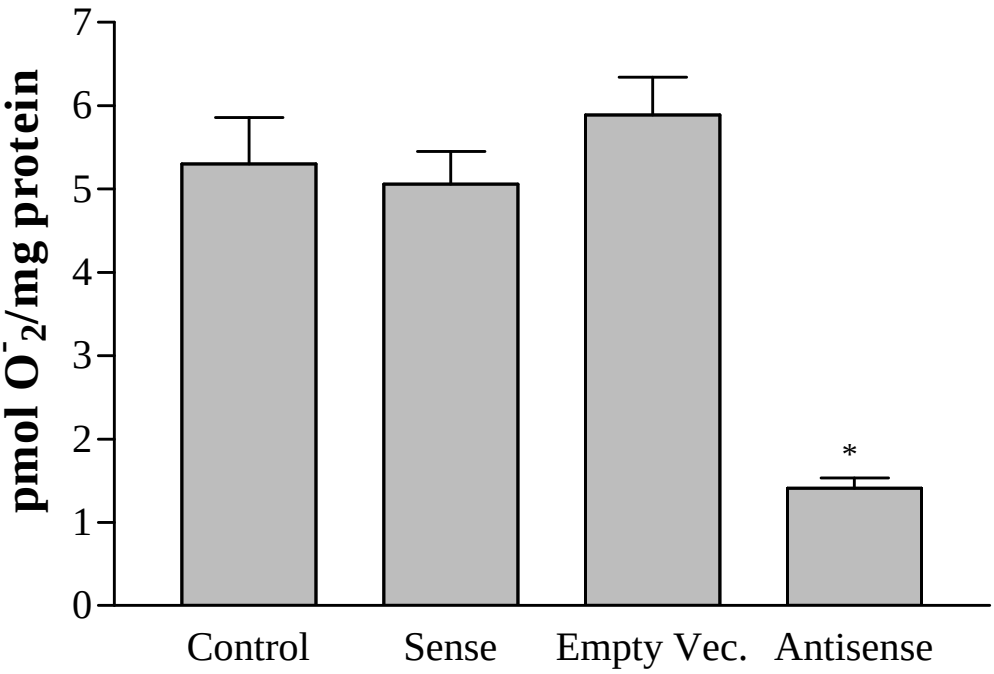
pmol O^-_2/mg protein
0
1
2
3
4
5
6
7
*
Control
Sense
Empty Vec.
Antisense

B

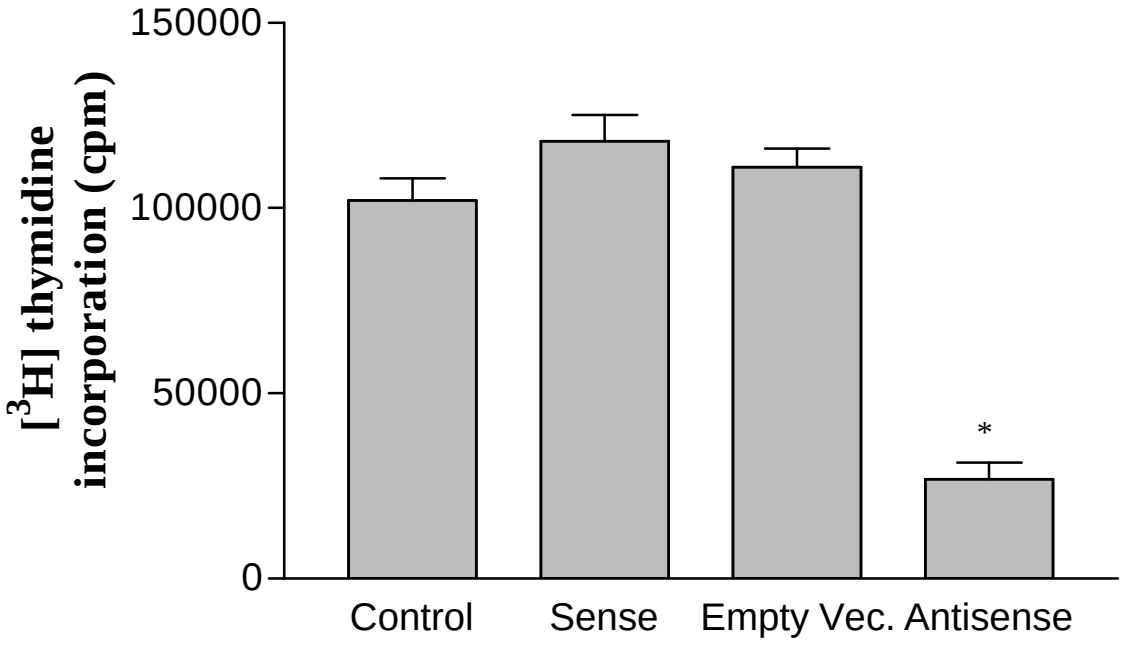
[^{3}H] thymidine incorporation (cpm)
0
50000
100000
150000
*
Control
Sense
Empty Vec.
Antisense